Authors

Gary Le

Kersey Manliclic

Duy Nam Ton

Author profiles begin on page 22

Key Terms

- Blade design
- Efficiency
- Experimental
- Power Output
- Savonius Wind Turbine (SWT)
- Vertical-Axis Wind Turbine (VAWT)
- Wind Energy

An Experimental Study on the Savonius Vertical-Axis Wind Turbine for Regions with Low-Speed Winds

Gary Le, *Mechanical Engineering*   **Duy Nam Ton,** *Mechanical Engineering*

Kersey Manliclic, *Materials Science Engineering & Mechanical Engineering*

Abstract

Traditional horizontal-axis wind turbines are usually designed for areas with naturally high-speed winds, but exhibit low performance when under low-speed wind. Vertical-axis wind turbines (VAWTs) provide an alternative that can be used in low-wind conditions. The objective of this study was to investigate the potential of VAWTs for harvesting wind energy from slow-moving wind by considering various blade designs. Field testing was conducted to investigate the effects of blade number and configuration and determine if it were possible to produce greater efficiency for power generation than the recirculation effect seen in traditional Savonius turbines. The results suggested that the power generated is sufficient to meet the energy demand if implemented appropriately.

Faculty Mentor

Fossil fuels are the major energy source supporting the rapid industrialization and economic growth in the past century. However, it is clear that they cannot sustain a global economy. Wind energy provides an alternative source for renewable energy. This paper investigates the performance of vertical wind turbines developed by the Wind Energy senior design project team in 2009–2010. The study has revealed the dependence of efficiencies on several factors, such as the blade configuration, and explored the optimal wind turbine design. The encouraging results provide both insights into modern wind turbine design and guidelines for future UCI Wind Energy teams. In 2010–2011, the team has developed a larger-scale wind turbine and is planning to install it over the Engineering Tower.

Yun Wang
Henry Samueli School of Engineering

Introduction

According to the Energy Information Administration (EIA), wind generated 0.34% of the nation's total energy consumed in 2007. Though this value may appear low at first, it was approximately the same percentage of energy provided by geothermal and much larger than the energy captured by solar photovoltaics (0.08%) ("U.S. Energy Consumption"). The major advantages of wind energy are that wind is not exclusive to any particular region in the world and its use emits no greenhouse gas. Furthermore, unlike natural gas or hydrogen, it provides a direct form of energy, not requiring the intermediate steps of extracting or manufacturing a fuel. It may be intuitive to assume that harnessing low-speed wind would generate much less power than high-speed wind. However, when considering land use, the logic becomes clear. For instance, as stated by the EIA, areas of high wind speeds within the U.S. are typically in the remote regions of the Midwest. Delivering the power captured from turbines placed in those parts of the country across far distances to populated suburban areas would result in an inefficient loss of energy. However, vertical-axis wind turbines could be placed in such suburban areas to capture local low-speed winds. In effect, there is a trade-off between power produced from high-speed winds and power lost during transport.

Savonius wind turbines (SWTs) are vertical-axis turbines that use two halves of a cylinder that form opposite facing scoops as pictured in Figure 1. SWTs operate under the drag principle in which the concave profiles of the blades are used to capture wind. However, SWTs generally have low efficiency compared to other turbines that use the lift principle. Lift occurs where a portion of the wind captured by the blades slightly elevates the rotor. The lifting causes the rotor to 'hover' in a low friction setting. Since the invention of SWTs, much research has been conducted to verify Savonius' claim of his turbine's theoretical maximum power coefficient of 0.35. Johnson discusses several experiments that were designed to verify this value (Johnson, 2001). Researchers at Kansas State University attained efficiencies of 35% to 40% with a turbine 2 meters tall and 1 meter in diameter. In addition, researchers at Sandia National Laboratories tested a turbine with a height of 1.5 meters and diameter of 1 meter which achieved a maximum efficiency of 25% (Johnson, 2001). University of Illinois researchers built several Savonius turbines with varying blade designs, achieving a maximum efficiency of 35%. A few groups attempted to improve the Savonius turbine's efficiency through cutting-edge methods. One such group was Hussain *et al.* (2008), who conducted a CFD (computational fluid dynamic) analysis on the efficiency of the Savonius wind turbine (SWT) and considered blades at various angles. They concluded that the most efficient angle of twist was 45 degrees, which exhibited a maximum efficiency of 33.85% compared to 25.6% without twisting. These studies verified that the Savonius turbine had great potential in low wind speed areas with an efficiency comparable to that of a horizontal axis wind turbine.

Following these experiments, we built a small-scale experimental SWT with adjustable blades and conducted testing at the top of the Engineering Parking Structure on the UC Irvine campus. The wind speed and power output were measured using a voltmeter and an anemometer with data acquisition capabilities for recording the data to a computer. The data from the tests was used to calculate the efficiency and compare the turbine to that of traditional SWTs. The data provides valuable information for harvesting wind energy in Southern California.

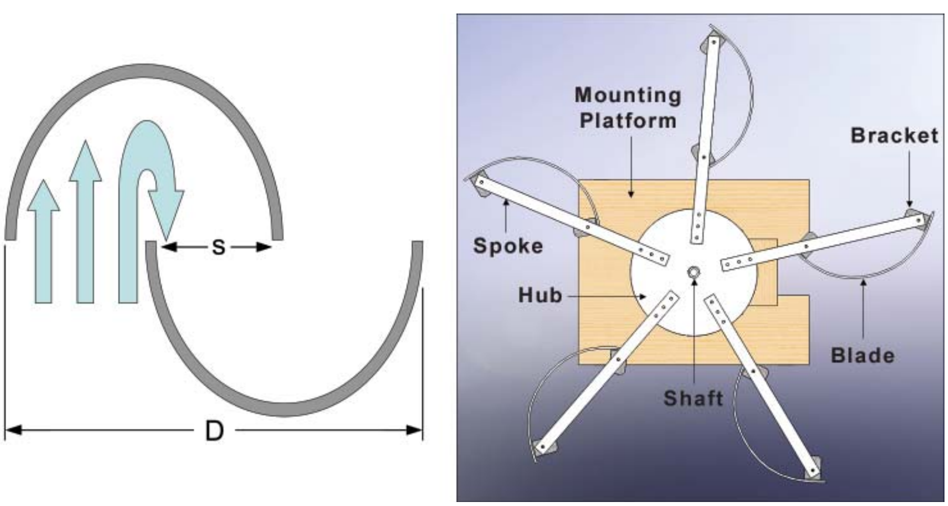

Figure 1

The top views of a traditional Savonius turbine with overlap S (left) and the modified VAWT rotor components on support mount (right).

Fabrication and Experimental Work

To investigate VAWT performance experimentally, we first designed and fabricated a small-scale VAWT. A field study was conducted and data was analyzed.

VAWT Design and Fabrication

According to literature, previous experiments on SWTs determined the optimal overlap ratio (G) to be 0.15 (Sargolzaei, 2007). G (s/D) is the ratio of overlap length, s, to diameter, D, of a turbine. Figure 1 shows the top view of a traditional double-bladed Savonius turbine with overlap distance (s). Flow analysis of this turbine showed that this gap allows wind to recirculate and provide additional torque to the other blade on the concave side. In contrast, our turbine has an open area in the center of the turbine to allow wind to pass through. It eliminates the recirculation of air in a traditional SWT. This modification may have decreased the efficiency of the turbine; however, the addition of extra blades was intended to provide compensation for this loss. Figure 1 (right) is the top-view computer-aided design (CAD) image of the rotor design. Both the number of blades and the blades' curvature were adjustable. A gearbox was developed to match the usually slow rotor spin with the RPM requirement of the generator.

Material Selection. Materials were selected to avoid structural failure of the wind turbine due to the forces that winds would impose on the blades. The drive shaft carried the most stress in this system due to the torsion produced by the blades and resistance in the gearbox. The hub and the spokes were made from 6061-aluminum alloy. Aluminum was chosen because it is relatively corrosion resistant, lightweight, easy to machine, and has sufficient strength. The five blades, drive shaft, and angle brackets were made of galvanized steel. The high strength of steel allowed the components to withstand mechanical failures such as shearing and torsion.

The Quantity of Wind Turbine Blades. The number of blades used for the wind turbine was determined mathematically. The optimal design choice would be the blade quantity that resulted in the largest exposure of blade area towards the wind—called the projected area. Because the blades are arranged equally in a circle, the projected area could be calculated by finding the angle of separation between the blades and the dimensions of the rotor. However, since the rotor spins, the projected area would change accordingly.

To illustrate how the blades' orientation affected the projected area, a two-blade design can serve as an example, with the blades spaced 180 degrees apart. The blades' change in orientation, as they rotated, was examined in two possible extreme cases, as shown in Figure 2. In one case, the blades reach their maximum exposure when positioned perpendicular to the wind (Figure 2a); the other is the minimum projected area, i.e. when the blades are turned parallel towards the incoming wind (Figure 2b). All other orientations in between result in intermediary projected areas.

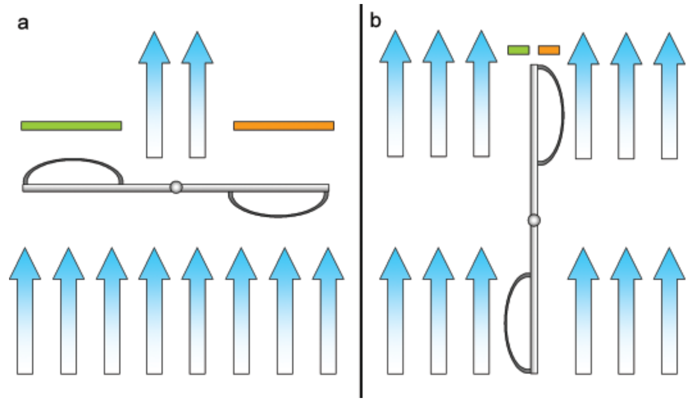

Figure 2

a) Two-blade design oriented orthogonal towards northward wind. b) Same design, but rotated 90 degrees, thus oriented parallel to wind. The blue arrows represent the wind, the green is projected profile and the orange is the backlash.

Table 1 and Figure 3 summarize the results obtained from the projected area calculations for different numbers of blades. Because the projected area changed with different orientations, the average value was recorded. Based on Table 1 and Figure 3, it was concluded that adding more blades increases the projected area. However, because the blades are spaced equally around the rotor, the angle between each blade decreases as more blades are added. Thus, the benefit diminishes because the rotor becomes cluttered and the blades block each other. Thus, the exposed area only increases diminutively as illustrated in Table 1 and Figure 3.

Table 1

Exposure areas at various blade numbers.

Blade Number	Degrees of Separation among Blades	Average Projected Area (in^2)
2	180.00	216.00
3	120.00	374.11
4	90.00	368.76
5	72.00	410.88
6	60.00	403.06
7	51.43	421.16
8	45.00	415.54
9	40.00	425.43
10	36.00	421.42

Based on the analysis summarized in Table 1 and Figure 3, five is the optimal number of blades to be integrated into

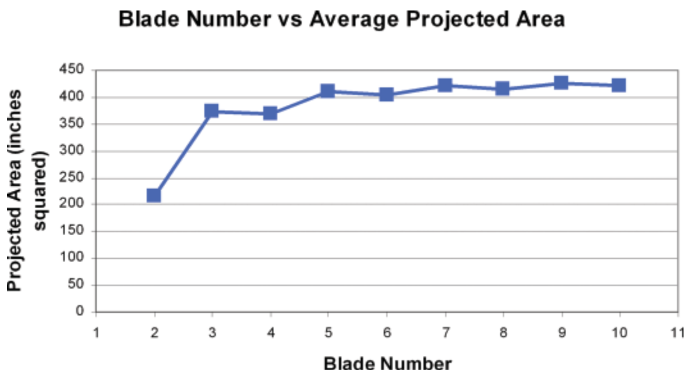

Figure 3

Exposure area exhibiting diminishing returns as blade number increases.

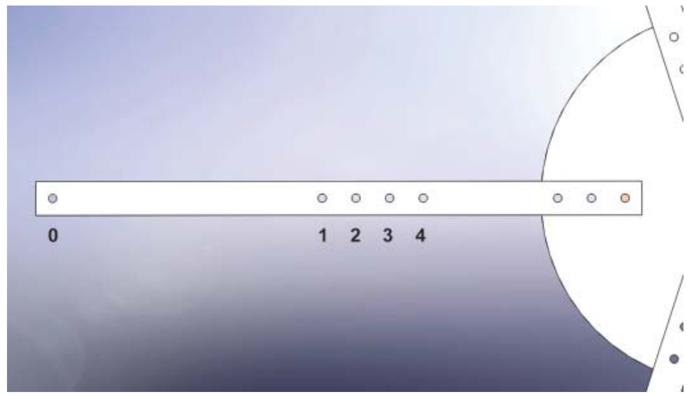

Figure 4

Top-view close-up of one VAWT Spoke.

the rotor design. Adding additional blades would result in a heavier rotor which might considerably lower its efficiency.

Blade Curvature Design. The blade design shown in Figure 2a favors a clockwise rotation. However, the incoming wind will also propel the blade on the right, causing the rotor to produce a torque counter-clockwise, against the favored rotation, resulting in a phenomenon known as backlash. The projected area that contributes to backlash is shown in orange in Figure 2. It is critical to note that the wind approaching the blade on the left will produce a drag force exceeding the backlash force produced by the blade on the right. The difference in drag force occurs because the wind blowing towards a concave profile will experience more drag than the portion of the wind approaching a convex profile. However, the directional bias of the rotor depends on the curvature of the blades rather than the quantity of blades. In determining the ideal number of blades, it was not important to consider the curvature of the blades as long as the width of the blade was held constant for every different blade quantity examined.

In determining the optimal curvature of the blades, the quantity of blades was held constant at five while the blade curvature profile was varied. The optimal blade curvature was to be determined experimentally. Therefore, the turbine had to be designed such that the blades could easily be adjusted to many different curvatures.

Figure 4 is a diagram of a top-view of the rotor with several holes drilled at different locations along the spoke in order to attach the blades to it. One end of the blade was to be held fixed (position 0) while the other end could be placed in any of the holes (position 1, 2, 3, or 4) to change the blade curvature.

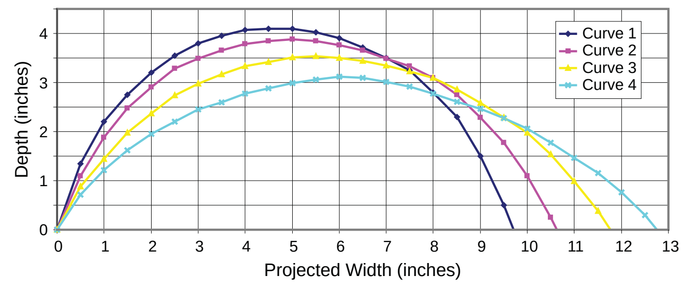

Figure 5

Resulting blade curvature when affixed to corresponding hole on spoke.

The contour of these curvatures could be precisely represented by 4th-order polynomial equations. The mathematical characteristics of each resulting curvature are summarized in Table 2 and plotted in Figure 5.

Gearbox Design. After the rotor was fabricated, the next task was designing the gearbox. From the graph in Figure 6, one can see that the amount of voltage produced is proportional to how fast the input shaft to the generator is spun (in RPM). The function of the gears is to increase the RPM delivered into the DC generator. By meshing gears, the

Table 2

Mathematical Parameters of Blade Curvatures.

Hole Position	Characterizing Equation; y =	Projected Width (Inches)
1	$-3\times10^{-5}\bullet x^4 + 0.0031\bullet x^3 - 0.1285\bullet x^2 + 2.5269\bullet x + 1.1418$	9.66
2	$-2\times10^{-5}\bullet x^4 + 0.0018\bullet x^3 - 0.0881\bullet x^2 + 2.0515\bullet x + 1.1189$	10.59
3	$-8\times10^{-5}\bullet x^4 + 0.0009\bullet x^3 - 0.0533\bullet x^2 + 1.5375\bullet x + 0.4494$	11.72
4	$-4\times10^{-5}\bullet x^4 + 0.0005\bullet x^3 - 0.0368\bullet x^2 + 1.2306\bullet x + 0.4142$	12.73

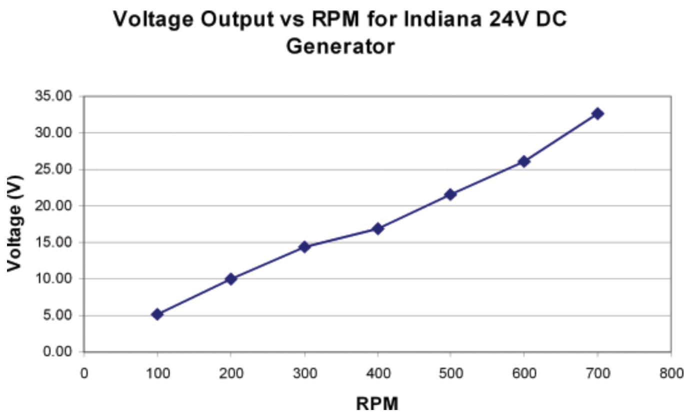

Figure 6

Electrical output of Indiana 24V DC motor when used as a generator.

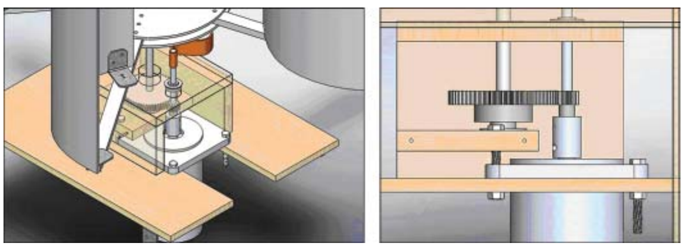

Figure 7

Rotor drive shaft is fixed to a large gear, which meshes with a smaller gear that is affixed to the generator's input shaft.

RPM delivered into the generator increases; however, this also requires a proportional amount of torque. Since the dimensions of the rotor were known and the wind speed could be measured, the amount of torque the rotor delivers under local wind conditions could be calculated. From the torque calculations, an allowable gear ratio of 1:5 was determined, made by meshing a 60-teeth spur gear with a 12-teeth spur gear. As a result, for every single rotation that the rotor made, the input shaft from the generator would rotate five times. Thus, the amount of power generated by using gears was five times greater than if the rotor were directly driving the generator shaft. A diagram of how the gears were meshed with respect to the drive shaft and DC generator is shown in Figure 7.

The VAWT Assembly. Figure 8 shows the actual turbine with a height of 60 inches, or 89 inches with the supporting mount. This size allows the turbine to be operated in any location without any obstruction and to be installed by hand without heavy machinery. On a commercial scale it could be operated in series on rooftops or highway dividers to provide energy for buildings and streetlights. This could potentially reduce the energy demand on power plants. Further research must be conducted to assess the practicality of implementing this type of wind turbine in large quantities.

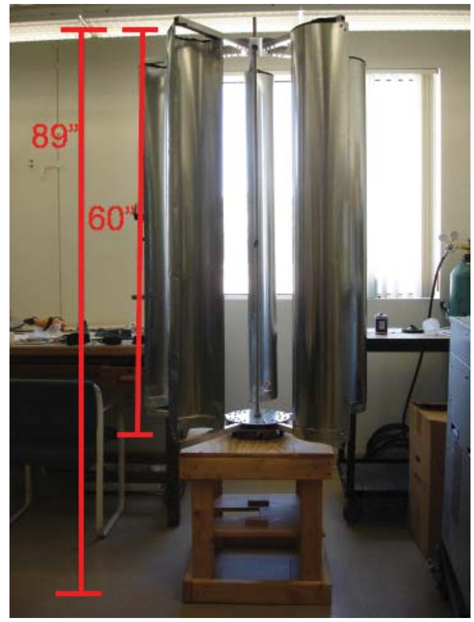

Figure 8

Photograph showing the size and scale of the wind turbine.

Experimental Testing and Data Processing

After the gearbox was fabricated and incorporated into the turbine assembly, the fully functioning system was ready for testing. The wind turbine testing was done on the rooftop of a six-story parking structure, where wind speeds and electrical power output from the VAWT could be measured. After data was collected, a correlation between the mechanical power input and electrical power output was graphed. The actual power output from the VAWT was compared with a theoretical power output, and these values were used to calculate the wind turbine's efficiency (Equation 1). The testing and analysis procedures were repeated for each different curvature. The efficiency value obtained from each curvature was used to determine which blade design was most favorable.

$$C_p = \frac{P}{P_w} \qquad (1)$$

Theoretical power (P_w) is the power that the turbine can capture from the wind (4).

$$P_w = \frac{1}{2}\rho A u^3 \qquad (2)$$

where ρ is the air density, u the wind speed, and A the projected area of the rotor.

Measuring Wind Speeds. The wind speeds were measured with an Extech HD-300 Digital Anemometer connected to a computer with a USB cable. Included with the anemometer was software that recorded the wind speed at a sampling rate of one data point per second.

Measuring Power Output. The power was calculated from Equation 3, where R is the resistance (Ω, Ohms) and V is the measurable voltage (Volts). To use Equation 3, the positive and negative terminals from both the DC generator and multimeter were joined to the ends of a 5 Ω resistor, as shown in Figure 9.

$$P = \frac{V^2}{R} \quad (3)$$

A MAS-345 Intelligent Digital Multimeter was used to measure the voltage output at those terminals. Like the anemometer, the multimeter also came with software that allowed continuous data acquisition. In order to synchronize the voltage data with the anemometer data, the sampling rate of the multimeter was also set to one data point per second.

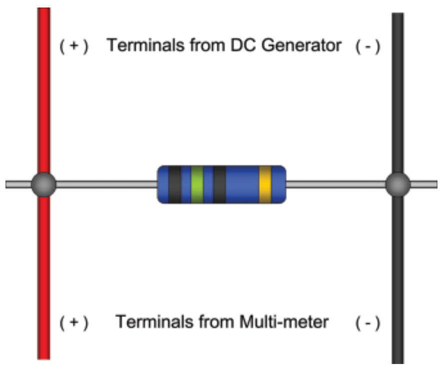

Figure 9

The setup for measuring power.

Results and Discussion

Figures 10 through 13 indicate that this design retains its self-starting ability. The cut-in speed—the speed at which the turbine instantaneously generates electrical energy—can be observed by looking at the first data point that has a power output greater than 0 volts, which is marked in red. According to the figures, the cut-in speed decreases with increasing curvature up until Curvature 3. Increasing to the fourth curvature, however, has a negative effect, resulting in a higher cut-in speed. The cut-in speeds are 1.59, 1.36, 1.29, and 1.38 mph, respectively, with increasing curvature. These results show that with increasing curvature, the blades have a larger frontal area that can capture more wind, but that increasing the curvature beyond the third has a negative effect. Keep in mind that the differences between these values are marginal when compared to the typical cut-in speed of the most efficient HAWT, which is reported to be approximately 8 mph.

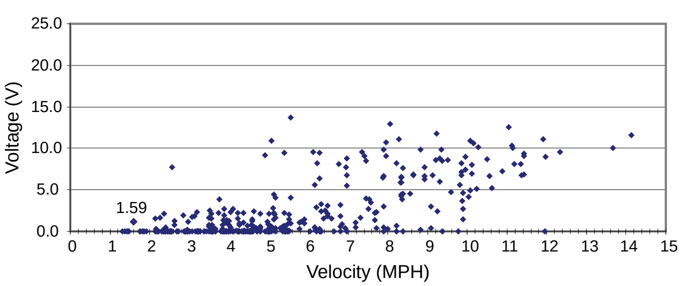

Figure 10

Cut-in speed for Curvature 1.

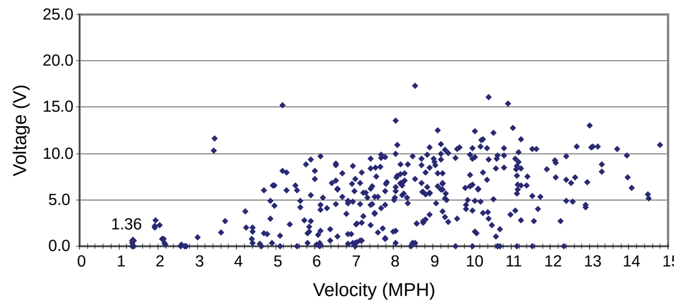

Figure 11

Cut-in speed for Curvature 2.

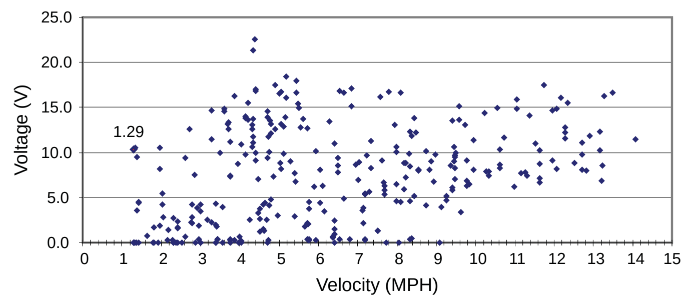

Figure 12

Cut-in speed for Curvature 3.

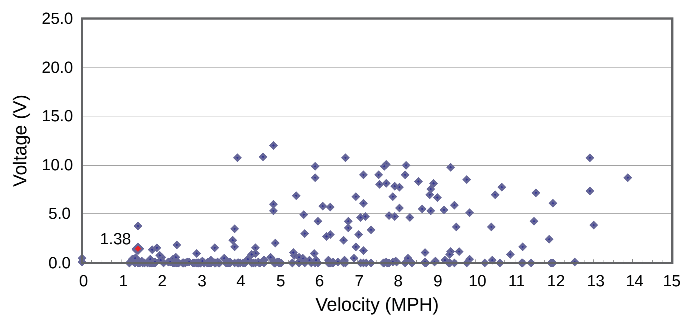

Figure 13

Cut-in speed for Curvature 4.

Figures 13 to 17 show a positive correlation between power output and curvature, with efficiency increasing with greater curvature. Figure 13 shows the first curvature's peak power output to be approximately 40 Watts compared to 105 Watts for the third curvature. Because this type of turbine relies on drag force to drive the rotor, a higher drag coefficient on the concave side of the blades in relation to the convex side corresponds to higher torque and better efficiency.

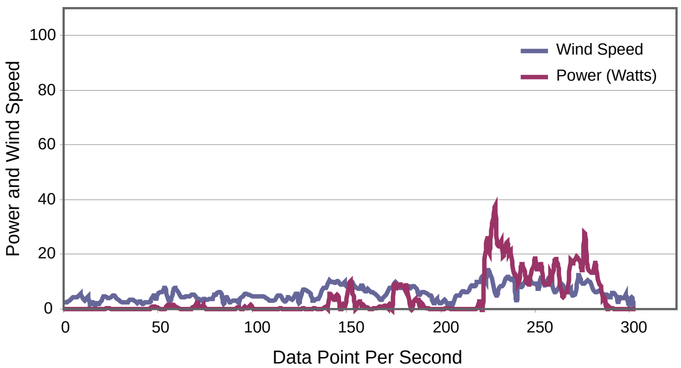

Figure 14

Power output relative to wind speed for Curvature 1.

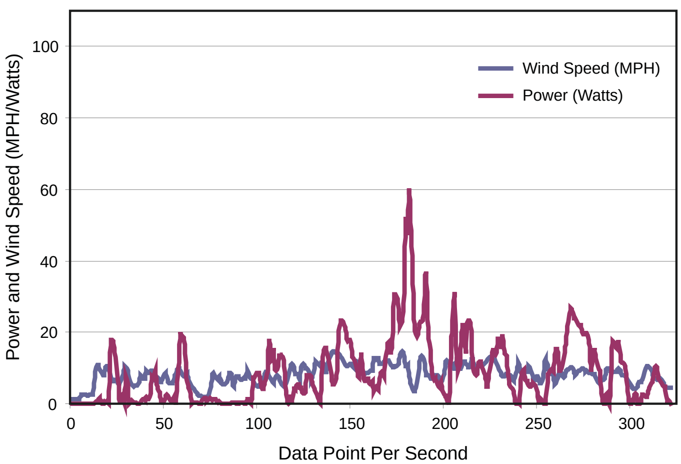

Figure 15

Power output relative to wind speed for Curvature 2.

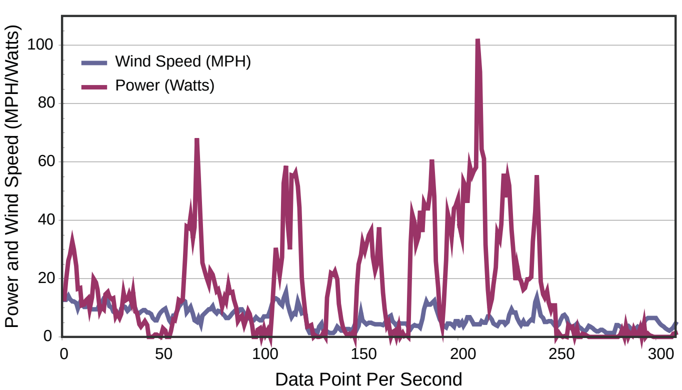

Figure 16

Power output relative to wind speed for Curvature 3.

The power coefficient is calculated using Equation 1, which yields the power coefficient equation (Cp). This value determines how efficient the wind turbine is according to the data. Curvature 3 is the most efficient with a value of 0.1984, which is only marginally greater than 0.1958 for Curvature 2, but much higher than 0.1002 and 0.1180 for

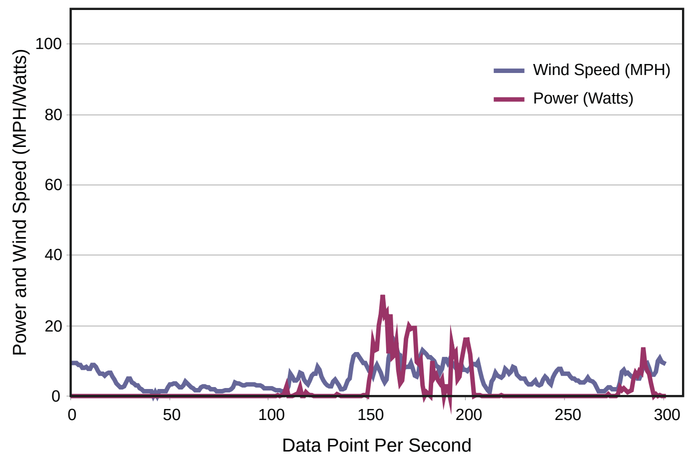

Figure 17

Power output relative to wind speed for Curvature 4.

Curvatures 1 and 4, respectively. From these Cp values, we can assume that this design is relatively less efficient than the traditional Savonius turbine with a reported Cp of 0.29 to 0.35. However, this design has two significant differences from the traditional design in that it has more blades and shorter curvatures, resulting in the loss of recirculation. Because the naturally occurring wind varies significantly, the readings are expected to vary proportionally.

Ideally, tests should be conducted in a wind tunnel for better control over wind speed and temperature. In addition, there were outlier data points where the measured power exceeded the Betz's Limit of 0.59; this limit is the theoretical maximum efficiency of a wind turbine. Therefore, data points greater than Betz's Limit were deleted because they are skewed data points that can affect the average Cp value. These skewed data points also show that the testing method contained errors, including those caused by the anomalous wind. This causes the constant, irregular stopping and starting of the rotor, resulting in inefficient readings of the voltage generated.

Conclusion

In this study, we designed and fabricated a small-scale experimental VAWT with adjustable blade designs. The VAWT was tested at the top of a tall parking structure at UC Irvine. The data suggested that the lowest wind speed for a turbine with curvature 3 and a diameter of 12 inches to produce power is 1.29 mph. This was also found to be the most efficient of the tested curvatures, producing a maximum efficiency of 19.84%, slightly less than the efficiency reported from literature, with a range of 25–45%.

Configuring the turbine with the third curvature, we found the average power output to be approximately 17 Watts. This is equivalent to 61.2 kWh/day, which is enough to power several appliances such as refrigerators and dishwashers. This kind of power output, however, is only possible with the wind at a constant 10 mph. Still, maintaining a rate of 15–20 kWh would be sufficient to offset the average energy usage for an American home—estimated to be around 30 kWh/day (EIA). This shows that wind energy is a viable alternative energy option for Southern California when coupled with other energy sources. Factors that can affect the viability of wind energy in Southern California include issues such as its aesthetic effect on the landscape and the cost and maintenance, which can be more expensive than the energy it produces.

Future work should include computer modeling of the rotor to study its flow profile and predict its performance in terms of torque and power coefficient. The results of these analyses could provide a better understanding of the fluid dynamic characteristics of our wind turbine design. Ideally, CFD (Computational fluid dynamics) or neural network analysis could be performed to compare with the results from the testing performed with naturally occurring wind. Another viable method would be to fabricate a scale model of the turbine to test in a wind tunnel with controlled wind speeds and real-time flow profiles from smoke-dyed wind. These studies will significantly advance the possibility for the wide-spread implementation of vertical-axis wind turbines in the future.

Author Profiles

Gary Le

Gary, being an advocate of renewable energy, was interested in learning more about viable energies for the future. He joined Professor Wang's 2010 Wind Energy Team, hoping to learn proper engineering and researching methods. The experience from this project was crucial to Gary's pursuit of a career in sustainable energy, as he learned the complexities that come with designing, fabricating, and testing a wind turbine and the importance of being resourceful to overcome complications. Gary hopes to find a career in the field of environmental engineering where he can apply his knowledge and contribute to society in its pursuit of sustainable living.

Kersey Manliclic

Kersey was looking to gain engineering experience within the field of sustainable energy and was fortunate enough to find an open spot with Prof. Wang's wind energy project. Apart from the knowledge learned regarding wind turbine technology, the overall experience of conducting research helped him learn to manage the challenges of staying within a budget, securing materials, and preparing presentations of results. Kersey hopes to further expand upon his experience by joining research projects on other forms of renewable energy and someday working in a field combining engineering with earth science.

Duy Nam Ton

Duy joined Prof. Wang's wind energy project with the intent of practicing his love of computer aided design and machine theory while obtaining some background knowledge on the subject of renewable energy. Towards the end of the year, what he found most valuable about the research was the leadership experience and seeing an engineering project progress through the cycle of design, fabrication, and testing. Duy hopes to take what he has learned from UC Irvine and apply it to an engineering career closer to his home town.

Acknowledgements

The authors thank Professor Yun Wang and his graduate students Thomas Tran, Jeffrey Mishler, and Sung Chan Cho for their valuable advice. We also thank the other members of the UCI 2009–2010 Wind Energy Team MAE189 senior design project for their contribution: Sarah Oliver, Zhiou Yang, Phong Phan, Khoi Le, Ka (Eric) Hei Ng, Ryan Wong, Matthew Woo, Elliot Lewis-Sullivan, and Ivan Zhang. Finally, the authors thank the Henry Samueli School of Engineering and UCI Undergraduate Research Opportunity Program for providing this research opportunity.

Works Cited

Altan B.D. and M. Atilgan. "An experimental and numerical study on the improvement of the performance of Savonius wind rotor." Energy Conversion and Management 29 (2008): pp. 3425–3432.

Altan B.D., M. Atilgan, and A. Ozdamar. "An experimental study on improvement of a Savonius rotor performance with curtaining." Experimental Thermal and Fluid Science 32 (2008): pp. 1673–1678.

Alternatives to Transportation Fuels 2008. U.S. Energy Information Administration. April 2010. http://www.eia.doe.gov/cneaf/alternate/page/atftables/afv_atf.html#supplied

Blackwell B.F., R.E. Sheldahl, and L.V. Feltz. Wind Tunnel Performance Data for Two- and Three-Bucket Savonius Rotors. Category UC-60, 19977, pp. 1–105.

Eriksson S., H. Bernhoff, and M. Leijon. "Evaluation of different turbine concepts for wind power." Renewable & Sustainable Energy Reviews 12 (2008): pp. 1419–1434.

Fernando M.S.U.K. and V.J. Modi. "A Numerical Analysis of the Unsteady Flow Past a Savonius Wind Turbine." Journal of Wind Engineering and Industrial Aerodynamics 32 (1989): pp. 303–327.

Frequently Asked Questions: How much electricity does an American home use? U.S. Energy Information Administration. June 2011. http://www.eia.gov/tools/faqs/faq.cfm?id=97&t=3

Fujisawa N. "On the torque mechanism of Savonius rotors." Journal of Wind Engineering and Industrial Aerodynamics, Vol. 40, 1992, pp. 277–292.

Hussain M.M., S.N. Mehdi, and P.R. Reddy. "CFD Analysis of Low Speed Vertical Axis Wind Turbine with Twisted Blades." International Journal of Applied Engineering Research 3.1 (2008): pp. 149–159.

Johnson G.L. Wind Energy Systems. Manhattan: 10, Dec, 2001.

Lanzafame R. and M. Messina. "Design and performance of a double-pitch wind turbine with non-twisted blades." Renewable Energy 34 (2009): pp. 1413–1420.

Pope K., I. Dincer, and G.F. Naterer. "Energy and exergy efficiency comparison of horizontal and vertical axis wind turbines." Renewable Energy 35 (2010): pp. 2103–2113.

Renewable Energy Consumption by Energy Use Sector and Energy Source. U.S. Energy Information Administration. April 2009. http://www.eia.doe.gov/cneaf/solar.renewables/page/trends/table2.html

Resources. American Wind Energy Association. 1996–2009. http://www.awea.org/faq/wwt_basics.html#What%20is%20wind%20energy

Saha U.K. and M.J. Rajkumar. "On the performance analysis of Savonius rotor with twisted blades." Renewable Energy 31 (2006): pp. 1776–1788.

Sargolzaei J. "Prediction of the power ratio in wind turbine Savonius rotors using artificial neural networks." International Journal of Energy and Environment 1.2 (2007): pp. 51–55.

Sargolzaei J. and A. Kianifer. "Modeling and simulation of wind turbine Savonius rotors using artificial neural networks for estimation of the power ratio and torque." Simulation Modelling Practice and Theory 17 (2009): 1290–1298.

Sargolzaei J. and A. Kianifer. "Neuro-fuzzy modeling tools for estimation of torque in Savonius rotor wind turbine." Advances in Engineering Software 41 (2010): pp. 619–626.

Tabassum S.A. and S.D. Probert. "Vertical-Axis Wind Turbine: A Modified Design." Applied Energy 28 (1987): pp. 59–67.

U.S. Energy Consumption by Energy Source. U.S. Energy Information Administration. April 2009. http://www.eia.doe.gov/cneaf/solar.renewables/page/trends/table1.html

Wind. Renewables and Alternate Fuels. U.S. Energy Information Administration. April 2008. http://www.eia.doe.gov/cneaf/solar.renewables/page/wind/wind.html

Wind Resources on Federal Lands. U.S. DOE, Pacifici Northwest Laboratory. 1986. http://www.eia.doe.gov/cneaf/solar.renewables/page/wind/wind.gif